



ELSEVIER

Available online at www.sciencedirect.com

SCIENCE @ DIRECT®

Applied Surface Science 219 (2003) 338–346

applied
surface science

www.elsevier.com/locate/apsusc

Melting point lowering of thin metal films (Me = In, Sn, Bi, Pb) in Al/Me/Al film system

N.T. Gladkikh^a, S.I. Bogatyrenko^b, A.P. Kryshstal^{a,*}, R. Anton^c

^aV.N. Karazin Kharkov National University, 4 Svobody sq., Kharkov 61077, Ukraine

^bScientific Centre of Physics and Technology, Novgorodskaja 1, Kharkov, Ukraine

^cInstitute of Applied Physics, University of Hamburg, Jungiusstrasse 11, 20355 Hamburg, Germany

Received 2 July 2002; received in revised form 13 May 2003; accepted 13 May 2003

Abstract

The variation of the melting point of thin films (10–40 nm) of In, Sn, Bi and Pb between thick (100 nm) Al films was investigated using elegant differential technique. The layer systems have been prepared by subsequent condensation of the components on amorphous substrates in vacuum. A decrease of the melting point of several degrees has been found for the metals in question between Al films. The differential method enables us to refine the values of the eutectic temperature for Me/Al systems and, in particular, to reveal that the eutectic temperature for the Al/In alloy does not coincide with the melting point of In, as was supposed till now, but is lower by 0.8 °C. The results are discussed on the basis of a thermodynamic approach and evolution of the binary phase diagram of fusibility with decreasing film thickness.

© 2003 Elsevier B.V. All rights reserved.

Keywords: Phase transitions; Al alloys; Eutectic temperature; Transmission electron microscopy; Surface energy; Wetting; Aluminium; Bismuth; Indium; Lead

1. Introduction

Studies of melting point lowering in small particles and thin films have a long history. Presently, it is well ascertained that the melting point of nanoparticles both free and on amorphous substrates decreases with decreasing particle size. It is also known that the substrate material influences the melting point variation, which is determined by the nature of interaction forces between film and substrate [1–4]. The thermodynamic treatment, originated by Pawlow [1], takes

into account the increased role of the surface energy for nanoobjects, and is most widely used for explaining these results. Using this approach, it has been shown that, generally, for small samples of size d (where d is a particle diameter, or thin fibre or film thickness), the relative change of the melting point is determined by the expression

$$\frac{\Delta T}{T_s} = \frac{\Delta \Omega k}{\lambda d}, \quad (1)$$

where k is the form-factor equalling 6, 4 and 2 for a particle, a thin fibre and a film, respectively, λ the melting heat, and $\Delta \Omega$ the change of the specific surface energy under melting of a small sample [5]. Two ultimate cases are possible. If the sample is located either in vacuum or in a completely “non-wetted”

* Corresponding author. Tel.: +380-572-457589.

E-mail address: aleksandr.p.kryshstal@univer.kharkov.ua (A.P. Kryshstal).

solid matrix, then the $\Delta\Omega$ value under melting is determined by the equation: $\Delta\Omega = \sigma_s - \sigma_l > 0$ (where σ_s and σ_l are the specific surface energy values of solid and liquid phases, respectively), and therefore we get $\Delta T/T_s > 0$, that means a decrease of the melting point with size decreasing. Another case corresponds to the complete “wetting” of the solid matrix by the substance, and consequently the $\Delta\Omega$ value is expressed as: $\Delta\Omega = -(\sigma_s - \sigma_l) < 0$. Therefore, we get $\Delta T/T_s < 0$, i.e. the melting point increases with decreasing sample size. Later, other authors have studied the influence of size, shape and environment of the particles on the phase diagrams of fusibility and have got the relation identical to Eq. (1) [6].

Nanosized embedded particles have attracted considerable attention in recent times. Most interesting are particle–matrix systems with components that are almost insoluble in the solid state, and have a miscibility gap in the liquid state. But, the melting behaviour of nanoparticles embedded in a solid matrix (usually with the higher melting point) is more complicated. Different authors report conflicting results. Thus, for example, Saka et al. measured the increase of the melting point of In particles embedded in Al matrix using in-situ heating in an electron microscope [7]. Contrary to this, Sheng et al. report a lowering of the melting point in studies of ultra-fine In particles embedded in Al matrix, prepared by ball milling and mixing of corresponding binary powder mixtures with subsequent compacting and sintering [9,12]. A similarly controversial situation is observed for estimates of wetting angles in the In/Al system. We note that the majority of studies were performed for easy-melting metals like In, Pb, Sn, Cd and Bi in Al matrix and it is known that these metals form an eutectic with Al, which has the temperature and composition close to that of the easy-melting component. At the same time, it was established earlier that the eutectic temperature in condensed binary films decreases with decreasing film thickness [8]. We suppose that just the formation of the eutectic in the film–matrix system would define the sign of the melting temperature variation of the easy-melting component in an Al matrix.

The idea of this work is to consider along with the wetting criteria the interaction character between the particle and matrix substances, which may be described by the binary phase diagram of fusibility

and its evolution with variation of components in size.

2. Experimental

Layered systems of thin In, Sn, Bi and Pb films embedded in thick Al films have been chosen for this study from the following considerations. First, quantitative data of the variation of the melting point with size are available for free particles and partially continuous films of these metals [10,11]. Moreover, a virtual absence of solubility in the solid state, concomitant with the formation of an eutectic, which has a composition and temperature close to that of the easy-melting component, is a common feature of In, Sn, Bi and Pb with Al phase diagrams [13]. At the same time, the Sn–Al phase diagram is principally different from others. Whereas the phase diagram of In, Bi and Pb with Al show considerable segregation gaps, a Sn and Al form a simple eutectic with unlimited solubility in the liquid state.

Layered films are prepared in vacuum by subsequent condensation of the components from separate sources. This method has been proposed earlier [14] and was used for studies of contact melting phenomena in several binary systems [15]. We have modified it into a differential one that enables us to safely observe the slight melting point variations (<0.2 K) of the thin film of easy-melting component due to size effects, and to determine the influence of Al on the latter.

Series of experiments have been performed under similar deposition conditions. Their general scheme was as follows (see Fig. 1). The substrates (polished

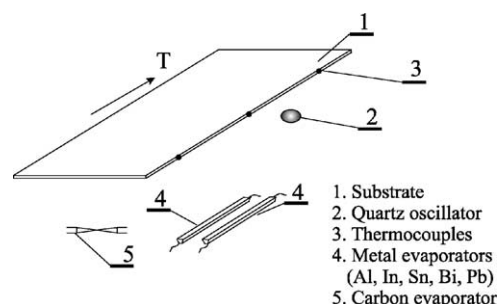


Fig. 1. Preparation scheme of layered film system by vacuum condensation.

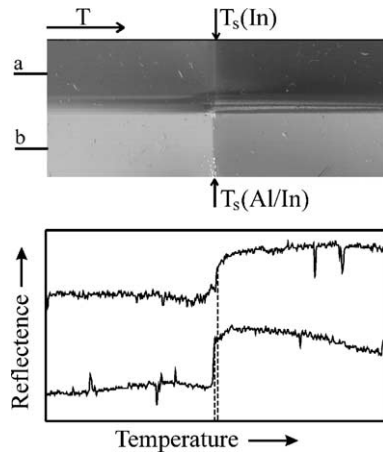


Fig. 2. Photograph of a substrate with thick Al/In alloy (a) and thick In film (b) and its photometric curves. Note the temperature shift between the Al/In eutectic temperature and the melting point of pure In.

stainless steel plates of size 30 mm × 150 mm × 3 mm) have been covered by 10 nm carbon film to avoid an interaction between the substrate and a system in question. The metals of 99.999% purity were evaporated from stripe molybdenum sources extended parallel to the long edge of the substrate. During deposition the vacuum was better than 10⁻⁴ Pa and the deposition rate was of the order of 3 nm/s in all experiments. The film thickness was monitored by a quartz oscillator, which was located near the middle of the substrate. The Al film thickness was 100 nm, while that of the other metal was varied. Typically, the substrate was covered in two halves along the long edge, with the layer system under investigation, and a reference system, respectively, e.g. Al plus the easy-melting metal, or the latter alone. To avoid any contamination of the Al/Me boundary the evaporation of Me starts just before the Al deposition was finished. Since the substrate was at room temperature, continuous films were formed, as was supported by electron microscopy images. After deposition, a temperature gradient was created along the substrate by heating one tip of the substrate. Upon melting of the easy-melting metal, clear boundaries were observed, corresponding to the melting point in both halves. The boundaries are formed due to the film morphology change upon melting [14,15]. The shift of the boundary with respect to the reference system enabled us to measure

the sign and magnitude of the difference between the melting points (see Fig. 2). The temperature gradient was 1 °C/mm and was created in such a way that the boundaries were located in the middle of the substrate, where the film thickness was measured. The temperature was controlled by three thermocouples (calibrated by melting of bulk Me films). Since the temperature gradient along the substrate was linear and was known we have measured precisely the distance between the melting boundaries of system in question and reference one and have calculated the difference between the melting points of these systems. The usage of special screen system enabled us to prepare on a single substrate up to seven (along its width) layered film systems with different compositions and thicknesses in a single experiment. One of the systems was used for a reference, which was either a thick (100 nm each) Me/Al double layer or a thick Me film alone.

Transmission electron microscopy was performed in a EM-125 microscope with 0.3 nm spatial resolution, operated at 125 kV and a Philips CM-12 operated at 120 kV. X-ray diffraction was conducted on a Dron-3M diffractometer with Cu K α radiation. The X-ray data were used for precise lattice constant measurements from diffraction peak positions as well as for elemental analysis.

3. Results

3.1. Eutectic temperature in Al/Me alloy

Since the literature controversially discusses the absolute values of the eutectic temperature of systems of Al with easy-melting metals, series of experiments have been performed, in which one part of the substrate was covered with an Al/Me double layer, whereas the pure Me was deposited on the other part. Such experiments allow us to determine the difference of the eutectic temperature from the melting point of the easy-melting component. The resulting values of the eutectic temperature were averaged from five to six experiments, and are compared with literature data in Table 1. Note that the proposed differential method yields refined values and, in particular, reveals that the eutectic temperature of the Al/In system does not coincide with the melting point of In, as was supposed

Table 1
Measured values of the eutectic temperature in Al/Me (Me = In, Bi, Pb, Sn) alloys and literature data

| System | Phase diagram type | Eutectic temperature, T_e (°C) | | Melting point of pure Me [13] (°C) |
|--------|--|----------------------------------|-----------------|------------------------------------|
| | | Experiment | Literature [13] | |
| Al/In | Eutectic with immiscibility area in liquid state | 155.6 | 156.4 | 156.4 |
| Al/Bi | Eutectic with immiscibility area in liquid state | 269.1 | 270 | 271 |
| Al/Pb | Eutectic with immiscibility area in liquid state | 325.3 | 327 | 327.4 |
| Al/Sn | Simple eutectic | 229.8 | 228.3 | 231.9 |

up to now, but is slightly lower it. This can be clearly seen in Fig. 2.

Since the experiments were performed in the vacuum of about 1×10^{-4} Pa, the formation of thin oxide layer may be possible. To check the influence of the latter on the eutectic temperature, we have changed the preparation sequence of layers. We did not find any difference between the eutectic temperatures in Al/In and In/Al alloys. Therefore, we have concluded that no oxide film at the Al/In interface is formed or, at least, there is no significant influence on the eutectic temperature of our systems. Fig. 3 shows the X-ray diffraction patterns of In/Al system before and after melting. No traces of any intermediate phase have been found. Measurements of the lattice constants resulted in $a = 0.4612$ nm, $c = 0.4935$ nm for In and $a = 0.4049$ for Al before melting (Fig. 3a), and $a = 0.4609$ nm, $c = 0.4936$ nm for In and $a = 0.4049$ for Al after melting (Fig. 3b). The

small decrease of c parameter of In after melting is probably caused by the slight solubility of Al in In.

3.2. Melting temperature in C/Sn/C system

According to the results of Morokhov et al. [5] an amorphous matrix should have no influence on the melting point of small-size samples, i.e. the behaviour of these particles should be similar to that of free ones. This assumption has been verified by experiments with thin Sn films on carbon substrates as well as embedded between two thick carbon layers (Fig. 4a). A continuous, straight boundary across both film systems is observed, which reveals that an amorphous carbon substrate does not influence the melting point of thin films (Fig. 5 shows the electron microscopy image of Sn droplets formed after melting of Sn film on a carbon substrate).

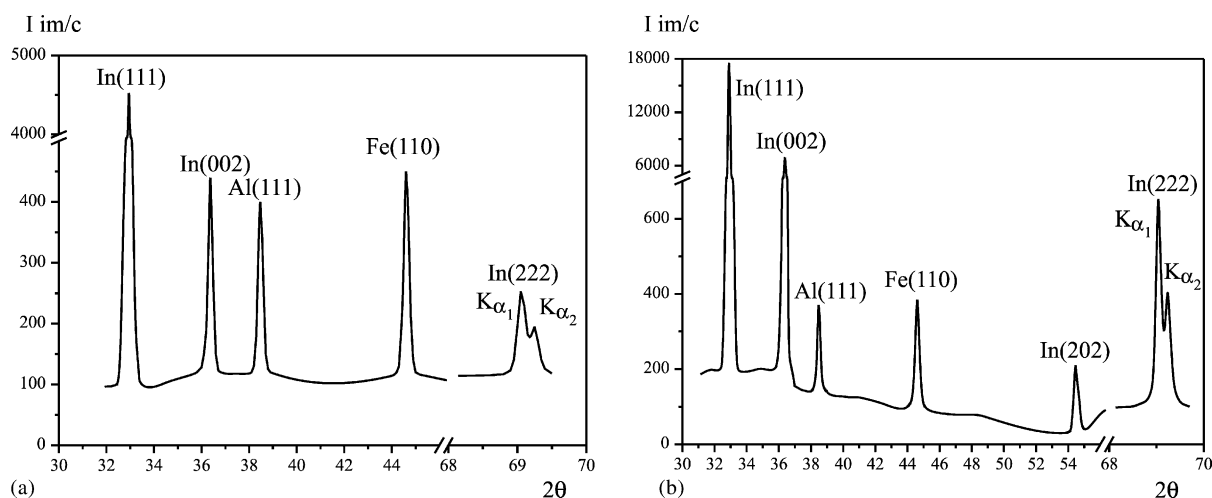


Fig. 3. X-ray diffraction patterns of In/Al system before (a) and after (b) melting.

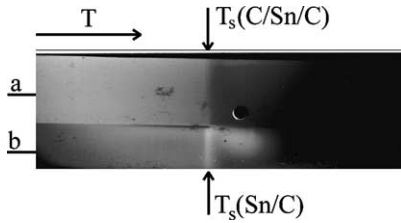


Fig. 4. Photograph of substrate with C/Sn/C (a) and Sn/C (b) film systems (Sn thickness is about 25 nm).

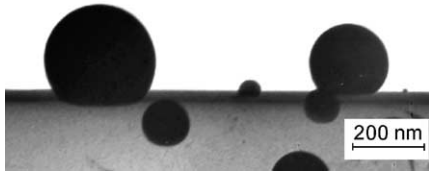


Fig. 5. Electron microscopy micrographs of Sn drops formed during melting of a continuous Sn film on the carbon substrate.

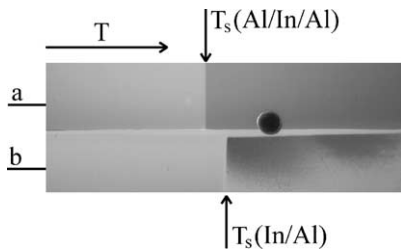


Fig. 6. Photograph of a substrate with thick Al/In/Al (a) and Al/In (b) film systems (In thickness about 25 nm).

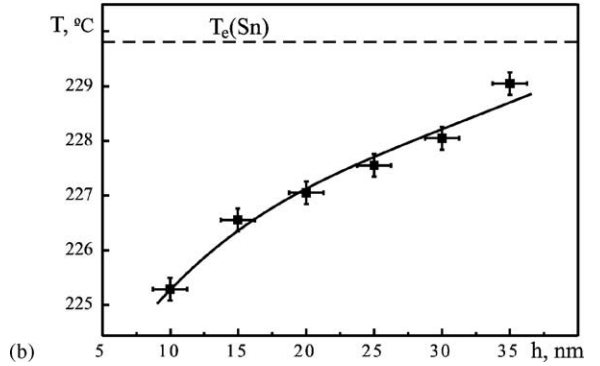
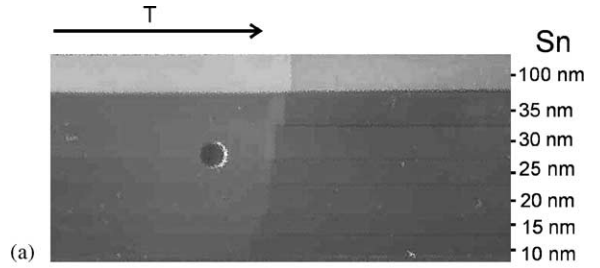


Fig. 7. Photograph of a substrate with a set of Al/Sn/Al film systems with different Sn film thicknesses (a) and corresponding plot of the eutectic temperature T vs. Sn film thickness h (b).

3.3. Melting temperature in Al/Me/Al systems

The melting points of thin films of In, Sn, Bi, and Pb embedded in Al were found to be lower than those of the pure metals. Also, the melting points decrease with decreasing thickness of these metals. This is clearly seen in Figs. 6 and 7, showing significant shifts of the melting boundaries. The sample shown in Fig. 7 contains seven parallel stripes of Al/Sn/Al film systems with different Sn thickness prepared in a single

Table 2
Measured values of the melting point of Me in Al/Me/Al film systems and comparison with literature data

| Metal in Al/Me/Al system | Experiment | | Small particles embedded in Al matrix [9] | | $\Delta T_h(3h/d)$ (°C) |
|--------------------------|------------|-------------------|---|-------------------|-------------------------|
| | h (nm) | ΔT_h (°C) | d (nm) | ΔT_d (°C) | |
| In | 25 | 3.5 | 15 | 16.9 | 17.5 |
| Bi | 20 | 5.0 | 22 | 14.6 | 13.6 |
| | 25 | 3.8 | | | |
| Pb | 30 | 3.0 | 13 | 20.5 | 20.7 |
| Sn | 20 | 3.0 | 17 | 12.1 | 10.6 |

Table 3
Calculated values of the wetting angles in Al/Me/Al film system and literature data

| Metal in Al/Me/Al system | Film system | | | Metal particles embedded in Al matrix [9] | | | |
|--------------------------|-------------------------------------|---|--------------|---|---|------------------|----------------------------|
| | $\Delta\Omega$ (mJ/m ²) | $\sigma_s - \sigma_l$ [18] (mJ/m ²) | θ (°) | $\Delta\Omega$ (mJ/m ²) | $\sigma_s - \sigma_l$ [18] (mJ/m ²) | θ [9] (°) | θ_{calc} (°) |
| In | 21.2 | 40 | 122 | 20.4 | 50 | 49 | 114 |
| Bi | 47.1 | 70 | 132 | 50.4 | 100 | 40 | 120 |
| | 45.0 | | 130 | | | | |
| Pb | 19.5 | 25 | 141 | 19.4 | 34 | 35 | 125 |
| | 26.6 | 30 | 151 | | | | |
| Sn | | | | 30 | 50 | 58 | 127 |

experiment. Results of the measurements are listed in Table 2 (columns 1–3).

4. Discussion

Since we have used continuous films in Al/Me/Al film systems, the results can be discussed on the basis of Eq. (1). However, it has to be taken into account that the variation of the surface energy upon melting is determined by the difference of the surface energies of the solid and the liquid Me film on the Al boundary, i.e. $\Delta\Omega = \sigma_{\text{ms}} - \sigma_{\text{ml}}$ (where σ_{ms} and σ_{ml} are the surface energies of the matrix–crystal boundary and the matrix–liquid film boundary, respectively). The σ_{ms} and σ_{ml} quantities can be estimated considering the equilibrium of liquid and crystal particles on the matrix surface assuming the invariability of wetting angle between surface (matrix) and particle upon their melting. This gives the relation

$$\Delta\Omega = \sigma_{\text{ms}} - \sigma_{\text{ml}} = -(\sigma_s - \sigma_l)\cos\theta. \quad (2)$$

The value of $\Delta\Omega$ was determined from the experimental data on the melting point lowering according to Eq. (1). The $(\sigma_s - \sigma_l)$ value in Eq. (2) represents the difference between the specific surface energies of solid and liquid phases at the temperature for which the $\Delta\Omega$ value has been calculated. These differences for metals under study are available in the literature in the wide temperature range [18]. Calculations of the wetting angle are performed for fixed metal thickness values according to Eq. (2). They resulted in angles $\theta > \pi/2$ for all systems (see Table 3, column 4). This result is also supported by electron microscopy studies of morphology and structure after melting, direct

measurements of wetting angles, and literature values [16] (see Fig. 8).

To compare literature results on melting of In, Pb, Sn and Bi nanoparticles embedded in Al matrix [9,12] with our results for thin films between thick Al films, we refer to the following ideas. According to Eq. (1), the ratio of the melting point lowering (ΔT_d) of the particle with diameter d embedded in a solid matrix to that of a thin film (ΔT_h) of thickness h between thick films (of the same material of the matrix) can be expressed as

$$\frac{\Delta T_d}{\Delta T_h} = \frac{3h}{d}. \quad (3)$$

Here we assume the form coefficient of a particle and a film to be equal to 6 and 2, respectively. These values follow from thermodynamic equilibrium of liquid and solid phases for nanoobjects of equal mass [5,20], and they were experimentally verified for Bi films in paper [21].¹ The values of ΔT_d for particles are calculated from our data ΔT_h for thin films according to Eq. (3). They are listed in Table 2, column 6 and are compared with data measured in paper [9] (Table 2, column 5).

From the data of Sheng et al. [9] we have also calculated the differences of the surface energies in solid and liquid state $\Delta\Omega$ for the case of a particle in an Al matrix according to Eq. (1) (Table 3, column 5), and have estimated the wetting angles for this case. All values of wetting angle exceed $\pi/2$ (Table 3, column 8). Similar results have been obtained for thin films in the Al/Me/Al layer systems (Table 3, column 4).

¹ It was experimentally found that upon melting of Bi continuous film it breaks in to spherical particles with a size $d = 3h$ (where h is the film thickness).

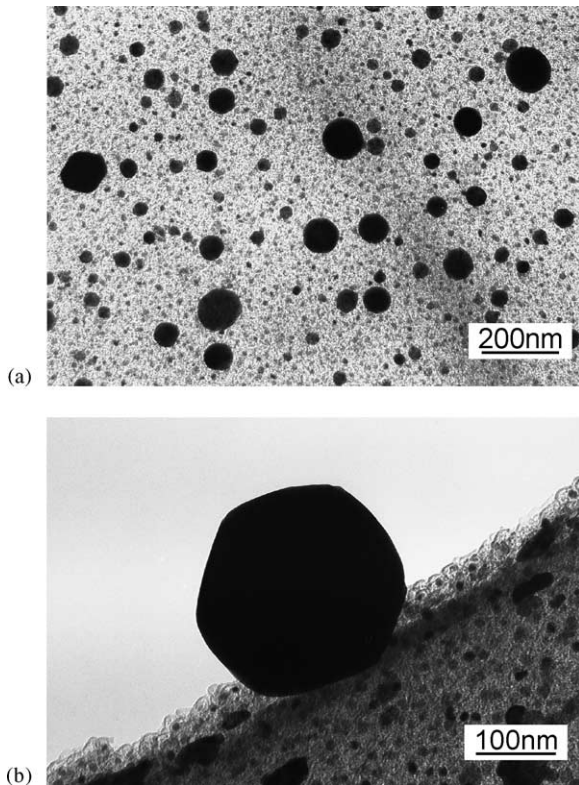


Fig. 8. Electron micrographs of Bi droplets formed during melting of continuous Bi film of 25 nm thickness in Al/Bi/Al system (a) and profile of crystallised Bi particle at the edge of an Al film (b).

In contrast, Sheng et al. [9] report wetting angles $\theta < \pi/2$ (see Table 3, column 7). The reason of the difference seems to be the following. The Sheng et al. [9] estimated the variation of the surface energy at the particle–matrix boundary upon melting using the assumption, that the crystal is not wetted ($\theta \neq 0$) by its own melt. But this is not the case for metals, where the crystal is completely wetted by its own melt, i.e. $\theta = 0$ [8].

Our results indicate that the behaviour of thin metal films in Al/Me/Al layered systems and of small particles embedded in Al matrix concerning the lowering of the melting point is similar to that of island films on non-wetted (wetting angle is $\theta \sim 120\text{--}130^\circ$) substrates. It is worth mentioning that the values of supercooling during crystallisation of In, Pb and Sn nanoparticles in an Al matrix reported by Sheng et al. [9] are significantly lower than those on non-wetted substrates. According to

the literature [17], the magnitude of the supercooling of Bi should be $\Delta T \sim 0.3T_s$ for a wetting angle of about 130° , which in fact agrees with that for Bi particles in an Al matrix obtained by Sheng et al. [9]. Significantly smaller values of supercooling during crystallisation of In, Pb and Sn particles in Al matrix are possibly caused by the catalytic effect of Fe particles, which got into the corresponding systems as a result of a long-time ball milling process.

All mentioned above indicates that there is insufficient to consider only the wetting character of matrix by the particle substance for explaining of the observed melting and crystallisation processes. Probably one should also take into account the character of the corresponding phase diagram and its evolution with the characteristic size changing.

The method of so called “geometrical thermodynamic” seems to be most suitable for our case. This method uses well-known statements of phase transition theory [19]. For a mixture of virtually pure components with complete insolubility the dependence of the free energy F on composition is given by the additivity rule, resulting in a straight line. If the components are completely soluble (unlimited solubility), the dependence of the free energy on concentration follows a smooth, continuous curve. The tips of this curve meet the y-axis and the second derivative $\partial^2 F/\partial x^2$ is positive for all values of x . Fig. 9 (upper part, solid lines) represents above dependencies for crystal and liquid phases for a two-component system with unlimited solubility of components in liquid state together with complete insolubility in solid state. Fig. 9 (lower part, solid lines) show the resulting diagrams of simple eutectic type for this case.

If we have small-size objects (small particles, thin films, etc.) we should include the surface energy, which may be considered as an additional contribution to the free energy of a system. This leads to a shift of the composition dependence of the free energy, e.g. for particle radius r , the specific free energy $F_r = F + (3\sigma_s/r)$ (broken lines in Fig. 9a) or for the film of thickness h , $F_h = F + (2\sigma_s/h)$ (broken lines in Fig. 9b). Since the surface energy of the liquid phase (σ_l) is smaller than of the solid (σ_s), the curves in Fig. 9a for constant particle size are shifted to lower temperatures when compared to the case of bulk. This shift would be the greater the smaller the size is. This is shown in Fig. 9a for the case of both components A

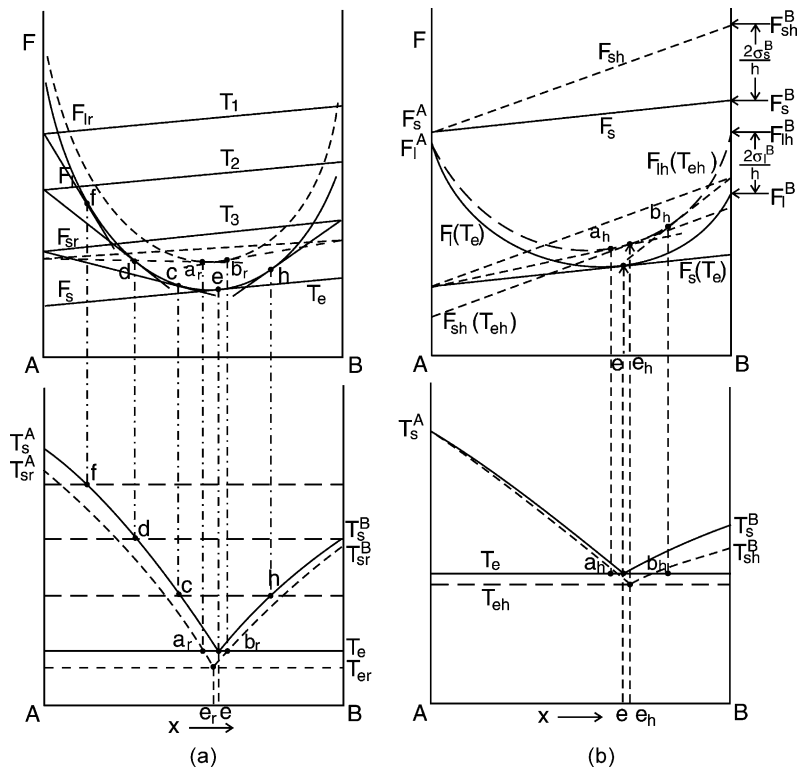


Fig. 9. Construction of phase diagram of simple eutectic type under complete insolubility of components in solid state. Broken lines in (a) are for the case when both components are small particles; broken lines in (b) are for the case when only one component (B) is a thin film of thickness h . Note the shift of the phase diagram to lower temperatures.

and B are in the form of small particles of radius r . Fig. 9b shows the case studied in the present work, namely only one component is in the form of a thin film of thickness h . One can see the corresponding asymmetric shift of the phase diagram to lower temperatures. It is obvious that in this case the shift of the eutectic temperature is smaller compared to one for two components being small-size objects. This fact has been explained in earlier work [8].

The measured shift in the studied systems is even smaller than the one from Fig. 9b, because the eutectic temperature in our systems is very close to the melting point of the easy-melting component. As a result, the eutectic temperature of studied systems is only slightly lower than that for thick films. This is clear from Fig. 2, which shows the photometric curves of corresponding Al/In film systems.

In real solid-state systems, some solubility, almost negligible, of the nanoobject's substance in the matrix exists [17] and, moreover, it is enhanced for small-size

objects as compared with bulk ones [8]. Naturally, this influences the interface energies of the particle–matrix system and affects the melting and crystallisation temperatures of small particles.

5. Conclusion

Our differential method of measuring melting points yields refined values of the eutectic temperatures for In, Bi, Pb and Sn with Al. We have shown that the melting points of In, Bi, Pb and Sn films between thick Al films decrease with decreasing thickness.

The observed lowering of the melting temperature in our layered film systems can be described on the basis of a thermodynamic approach taking into account the increased role of the change of the interface energy upon melting as well as of the evolution of the binary phase diagram of fusibility with decreasing film thickness.

References

- [1] P. Pawlow, *Z. Phys. Chem.* 65 (1909) 545.
- [2] M. Takagi, *J. Phys. Soc. Jpn.* 9 (1954) 359.
- [3] R. Bröll, K.G. Weil, in: R. Niedermayer, H. Mayer (Eds.), *Grundprobleme der Physik dünner Schichten*, Vanderhoeck & Ruprecht, Gottingen, 1966, p. 198.
- [4] N.T. Gladkikh, R. Niedermayer, K. Spiegel, *Phys. Status Solidi B* 15 (1966) 181.
- [5] I.D. Morokhov, S.P. Chizik, N.T. Gladkikh, L.K. Grigor'eva, *Soviet Phys. Dokl.* 23 (1978) 921.
- [6] M. Wautelet, *Effects of size, shape and environment on the phase diagrams of small structures*, *Nanotechnology* 3 (1992) 42.
- [7] H. Saka, Y. Nishikawa, T. Imura, *Philos. Mag. A* 57 (1988) 895.
- [8] N.T. Gladkikh, S.P. Chizhik, V.I. Larin, L.K. Grigor'eva, V.N. Sukhov, *Soviet Phys. Dokl.* 33 (1988) 362.
- [9] H.W. Sheng, K. Lu, E. Ma, *Acta Mater.* 46 (1998) 5195.
- [10] P.R. Berman, A.E. Curzon, *Can. J. Phys.* 52 (1974) 923.
- [11] V.P. Skripov, V.P. Koverda, V.N. Skokav, *Phys. Status Solidi A* 66 (1981) 109.
- [12] H.W. Sheng, J. Xu, L.G. Yu, X.K. Sun, Z.Q. Hu, K. Lu, *J. Mater. Res.* 11 (1996) 2841.
- [13] M. Hansen, K. Anderko, *Constitution of Binary Alloys*, McGraw-Hill, New York, 1958.
- [14] N.T. Gladkikh, A.V. Kunchenko, V.I. Lazarev, A.L. Samsonik, V.N. Sukhov, *Met. Phys. Adv. Technol.* 15 (1995) 280.
- [15] N.T. Gladkikh, A.V. Kunchenko, V.I. Larin, V.I. Lazarev, A.L. Samsonik, V.N. Sukhov, *Funct. Mater.* 6 (1999) 958.
- [16] S.P. Chizhik, N.T. Gladkikh, V.I. Larin, L.K. Grigoryeva, S.V. Dukarov, S.V. Stepanova, *Phys. Chem. Mech. Surf.* 4 (1987) 111.
- [17] N.T. Gladkikh, S.V. Dukarov, V.N. Sukhov, *Z. Metallkd.* 87 (1996) 233.
- [18] N.T. Gladkikh, S.V. Dukarov, V.I. Larin, *Funct. Mater.* 1 (1994) 49.
- [19] J.W. Christian, *The Theory of Transformations in Metals and Alloys*, Pergamon Press, Oxford, 1977.
- [20] M. Wautelet, *Nanotechnology* 3 (1992) 42.
- [21] N.T. Gladkikh, R.I. Zaichik, V.P. Lebedev, L.S. Palatnik, V.I. Khotkevich, *Surface Diffusion and Spreading*, Nauka, Moscow, 1969 (in Russian).